THE JOURNAL OF BIOLOGICAL CHEMISTRY VOL. 287, NO. 4, pp. 2666–2677, January 20, 2012

Inhibition of Signal Transducer and Activator of Transcription 3 (STAT3) Attenuates Interleukin-6 (IL-6)-induced Collagen Synthesis and Resultant Hypertrophy in Rat Heart[S]

Received for publication, March 31, 2011, and in revised form, November 18, 2011 Published, JBC Papers in Press, December 8, 2011, DOI 10.1074/jbc.M111.246173

Saiful Anam Mir[‡], Arunachal Chatterjee[‡], Arkadeep Mitra[‡], Kanchan Pathak[‡], Sushil K. Mahata[§], and Sagartirtha Sarkar[‡1]

From the [‡]Department of Zoology, University of Calcutta, 35, Ballygunge Circular Road, Kolkata 700 019, India and the [§]Department of Medicine, University of California, San Diego, La Jolla, California 92093-0838

IL-6 has been shown to play a major role in collagen up-regulation process during cardiac hypertrophy, although the precise mechanism is still not known. In this study we have analyzed the mechanism by which IL-6 modulates cardiac hypertrophy. For the *in vitro* model, IL-6-treated cultured cardiac fibroblasts were used, whereas the *in vivo* cardiac hypertrophy model was generated by renal artery ligation in adult male Wistar rats (*Rattus norvegicus*). During induction of hypertrophy, increased phosphorylation of STAT1, STAT3, MAPK, and ERK proteins was observed both *in vitro* and *in vivo*. Treatment of fibroblasts with specific inhibitors for STAT1 (fludarabine, 50 μM), STAT3 (S31-201, 10 μM), p38 MAPK (SB203580, 10 μM), and ERK1/2 (U0126, 10 μM) resulted in down-regulation of IL-6-induced phosphorylation of specific proteins; however, only S31-201 and SB203580 inhibited collagen biosynthesis. In ligated rats *in vivo*, only STAT3 inhibitors resulted in significant decrease in collagen synthesis and hypertrophy markers such as atrial natriuretic factor and β-myosin heavy chain. In addition, decreased heart weight to body weight ratio and improved cardiac function as measured by echocardiography was evident in animals treated with STAT3 inhibitor or siRNA. Compared with IL-6 neutralization, more pronounced down-regulation of collagen synthesis and regression of hypertrophy was observed with STAT3 inhibition, suggesting that STAT3 is the major downstream signaling molecule and a potential therapeutic target for cardiac hypertrophy.

Cardiac fibrosis is considered to be a major player during hypertrophy, where excess synthesis and a disproportionate accumulation of extracellular matrix proteins in the myocardium leads to its stiffness and diastolic dysfunction, leading to heart failure (1–3). Fibrillar collagen 1 and collagen 3 are the most abundant extracellular matrix proteins in the myocardium that maintain myocardial structural integrity (4). Collagen biosynthesis process is mainly compartmentalized in cardiac fibroblasts with a continuous turnover of newly synthesized collagen and degradation of old existing collagen, which involves post-transcriptional as well as post translational events. A physiological balance exists between collagen synthesis and degradation that is necessary to maintain tissue integrity of the myocardium. Extracellular catalytic cleavage of collagen is mediated by matrix metalloproteinases (MMPs)[2] that are eventually regulated by their naturally occurring endogenous inhibitors, *i.e.* tissue inhibitors of metalloproteinases (TIMPs) (1, 5).The fine balance between MMPs and TIMPs plays a crucial role in regulation of cardiac collagen turnover (5, 6). Furthermore, lysyl oxidase (LOX) is also instrumental during collagen biogenesis that catalyzes lysine-derived cross-bridges between two or more lysine residues of nascent procollagen peptides during their maturation into collagen molecules (5, 7). Altered and deregulated expression of these factors has been demonstrated in failing myocardium (5).

Involvement of various neurohumoral and growth factors has also been illustrated in the development of cardiac fibrosis both *in vitro* and *in vivo* (3, 8). Cellular cross-talk between AngII-treated cardiomyocytes and fibroblasts has been shown to play an important role during collagen up-regulation with involvement of IL-6 during fibrosis (8–10). Recently, Meléndez *et al.* (11) showed that IL-6 infusion in rats resulted in cardiac hypertrophy with considerable fibrosis within the myocardium. But the precise mechanism and involvement of key signaling molecules for collagen up-regulation process during hypertrophy is still unclear.

It is known that the IL-6 family of cytokines mediates their action primarily through the activation of Janus kinase signal transducers and activators of transcription (JAK-STAT) pathway along with other intracellular signaling pathways (12). The IL-6 family of cytokines mostly activates STAT3 and to a lesser extent STAT1 via a common receptor subunit (13). STAT proteins are also shown to be activated by interleukins indirectly through the activation of mitogen-activated protein kinases (MAPKs). STAT proteins have been shown to induce transcription of several genes involved in ischemia/reperfusion injury and pressure-overload hypertrophy, as well as in cardioprotection, angiogenesis, cell survival, and apoptosis (14–20). The present study was, therefore, designed to study the functional role of STAT proteins in IL-6-mediated collagen gene up-regulation *in vitro* and *in vivo*. This is the first report showing

[S] This article contains supplemental Tables 1 and 2 and Figs. 1–3.

[1] To whom correspondence should be addressed. Tel.: 33-2475-3681; Fax: 33-2476-4419; E-mail: sagartirtha.sarkar@gmail.com.

[2] The abbreviations used are: MMP, matrix metalloproteinase; TIMP, tissue inhibitors of metalloproteinase; AngII, angiotensin II; HW, heart weight; BW, body weight; NSsiRNA, nonspecific control siRNA; ANF, atrial natriuretic factor; β-MHC, β-myosin heavy chain; LOX, lysyl oxidase.

involvement of STAT3 in the IL-6-induced collagen up-regulation process during cardiac hypertrophy.

EXPERIMENTAL PROCEDURES

28-Week-old Wistar male rats used in this study were obtained from the National Institute of Nutrition, Hyderabad, India. This investigation was approved by the Institutional Animal Ethics Committee, University of Calcutta (Registration #885/ac/05/CPCSEA), registered under "Committee for the Purpose of Control and Supervision of Experiments on Laboratory Animals," Ministry of Environment and Forests, Government of India and conforms with the *Guide for the Care and Use of Laboratory Animals* published by the United States National Institutes of Health Publication 85–23, revised 1996.

Cardiac Fibroblast Culture and Treatment—Fibroblast cells were isolated from 28-week-old male rat hearts by the collagenase dispersion method (21). Briefly, animals were euthanized in a prefilled CO_2 chamber with 100% concentration of CO_2, and the hearts were cut into small pieces and digested by collagenase (80 units/ml DMEM; Worthington). The cells were pelleted by centrifugation and resuspended in fresh complete DMEM supplemented with 10% fetal bovine serum and plated in cell culture flask. Cells were maintained at 37 °C with 5% CO_2 and were subsequently passaged. 75–80% confluent serum-starved cells were treated for 24 h with 10^{-8} mol/liter (Sar^1)-Angiotensin II (Bachem) and 50 ng/ml murine IL-6 (Peprotech). In another set of experiments IL-6 was preincubated with neutralizing IL-6 antibody (Abcam; catalog #ab9770) for 1 h before using it to treat cultured cardiac fibroblasts. Time-dependent phosphorylation status of different signaling proteins by AngII or IL-6 treatment was also studied starting from 5 min onwards until 12 hr. AngII-treated cells were used as positive controls for all subsequent experiments. Untreated cells were used as controls.

Generation of Animal Model of Cardiac Hypertrophy—In vivo cardiac hypertrophy model was generated by ligating right renal artery of 28-week-old male rats (250–300 g; $n = 10$) as described earlier (22). Rats were anesthetized with an intraperitoneal injection of a mixture of ketamine (80 mg/kg) and xylazine (12 mg/kg). The right renal artery was tied with a silk suture after placing a stainless wire (outer diameter, 0.34 mm) along the artery. The wire was then removed from the knot, causing constriction of the artery equivalent to the diameter of the wire. Rats that underwent a similar procedure without aortic ligation were termed as sham-operated control group ($n = 10$). Animals were maintained in optimum condition for 14 days and were sacrificed on the 15th day after surgery. Hearts were taken out and either fixed in Karnovsky's fixative for histological study or stored in liquid nitrogen for future use. Hypertrophy was measured by the heart weight (HW in mg) to body weight (BW in g) ratio (23). For neutralization experiment, one group of ligated rats was administered with neutralizing IL-6 antibody (10 μg/day; Abcam; catalog #ab9770) intraperitoneally on alternate days after ligation until the day of sacrifice (24).

Determination of Cardiac Function—Two-dimensional echocardiography was performed to determine cardiac function *in vivo*. Lightly sedated renal artery-ligated and sham-operated rats on the 15th day after surgery were evaluated using the M-mode views on a transthoracic study, measuring left ventricular systolic and diastolic dimensions and fractional shortening (%). Data were correlated with timing of the QRS complex. Digitized images were obtained using an ultrasound system (VividS5 system, GE Healthcare).

Estimation of IL-6 in Fibroblast Culture Supernatant and Rat Blood Serum by ELISA—Secreted IL-6 content in the AngII-treated (24 h) fibroblast culture supernatant and circulatory IL-6 level in rat blood serum (on the 15th day after surgery) was estimated by ELISA using rat IL-6 ELISA Kit (Thermo-Scientific, IL) following the manufacturer's procedure. The amount of IL-6 in each sample was determined by interpolating the absorbance value against a standard curve, and values were expressed as picograms of IL-6 per ml sample (pg/ml).

Reverse Transcription PCR (RT-PCR) and Real Time RT-PCR—Total RNA from cells (24 h treatment) and tissues (on the 15th day after surgery) was isolated using TRIzol reagent (Invitrogen) following manufacturer's instructions. 1 μg of total RNA was used to make cDNA using the cloned avian myeloblastosis virus (AMV) first-strand cDNA synthesis kit (Invitrogen). RT-PCR was done for *collagen 1*, *collagen 3*, *MMP-2*, *MMP-9*, *TIMP-1*, *TIMP-2*, *LOX*, *GAPDH*, atrial natriuretic factor (*ANF*), β-myosin heavy chain (β-*MHC*), c-*fos*, c-*jun*, and c-*myc* using specific oligonucleotide primers (supplemental Table 1). Relative quantification of PCR-amplified products was also done by real-time PCR with Power SYBR Green^{TM} PCR Master Mix using ABI7500 (Applied Biosystems). *Collagen 1*, *collagen 3*, *MMP-2*, *MMP-9*, *TIMP-1*, *TIMP-2*, and *LOX* gene expressions were studied by real time PCR, and *GAPDH* was used as a reference gene to normalize expression of other genes (supplemental Table 2). All real time PCR reactions were done in triplicate after an initial incubation at 95 °C for 10 min and then a PCR cycle at 95 °C for 30s, 59 °C for 30s, and 72 °C for 30s for 40 cycles. Relative gene expression was quantified by comparative "ct" ($2^{-\Delta\Delta ct}$) method.

Estimation of Total Collagen by Hydroxyproline Assay—Hydroxyproline assay was performed to measure total collagen content both in renal artery-ligated ventricular tissue (on the 15th day after surgery) as well as in fibroblast culture supernatant (24 h treatment) (25). Briefly, the tissue samples and fibroblast culture supernatants were digested with 6 N hydrochloric acid overnight at 110 °C followed by vacuum drying of the samples. After resuspending the samples in citrate acetate buffer, a colored reaction was done by adding isopropyl alcohol, chloramine T, and Ehrlich's reagent. The samples were incubated at 25 °C for 18 h, and intensity of the red color was measured at 558 nm using Varioskan Multimode Reader (Thermo Fisher). With the help of a standard curve, hydroxyproline content in the unknown samples was calculated. The amount of collagen was calculated by multiplying hydroxyproline content by a factor of 8.2.

Western Blotting—Western blot analysis was done to study protein expression both *in vitro* and *in vivo* (26). 30-μg protein samples were separated in 10–12.5% SDS-PAGE and transferred to PVDF^{+} membrane. After blocking with 5% nonfat dry milk, membranes were incubated with antibodies to IL-6 (Santa Cruz), STAT1, STAT3, p38 MAPK, ERK1/2, phospho-STAT1-

Tyr-701, phospho-STAT1-Ser-727, phospho-STAT3-Tyr-705, phospho-STAT3-Ser-727, phospho-p38 MAPK, and phospho-ERK1/2 (Cell Signaling) in 5% BSA solution at 4 °C overnight. After washing, membranes were incubated with horseradish peroxidase-conjugated secondary antibodies (Pierce) at room temperature for 1 h. Finally, the signals were detected using a chemiluminescence detection kit (Millipore). Scanned autoradiography images were quantified using ImageJ software (NIH), and values were expressed in arbitrary units.

Treatment of Cardiac Fibroblasts with Inhibitors to STAT and MAPK Proteins—Treatment of cultured fibroblasts with IL-6 was done in the presence or absence of different STAT and MAPK inhibitors. Fludarabine (50 μM) (Aldrich), a specific STAT1 inhibitor, and S31-201 (10 μM) (Calbiochem), a STAT3 inhibitor, were used in this study (27, 28). SB203580 (Calbiochem) at a concentration of 10 μM and U0126 (Calbiochem) at a concentration of 10 μM were used to block p38 MAPK and ERK1/2 respectively (29). All the inhibitors were added 45 min before the treatment, except fludarabine, which was added 2 hours before treatment (27–29). Cells treated with equivalent concentration of DMSO were used as controls. IL-6 induction of cultured cells after inhibitor treatment was done for 20 min to check phosphorylation status of STAT3, STAT1, p38 MAPK, and ERK1/2.

Treatment of Cardiac Fibroblasts with STAT3 siRNA—STAT3 activity in cultured cardiac fibroblasts was also blocked by using a STAT3-specific siRNA. Cultured fibroblasts were transfected with 300 pmol of STAT3 siRNA (SI 02040731; Qiagen) using Lipofectamine 2000 reagent (Invitrogen) following the manufacturer's guidelines. 24 h after transfection cells were used for treatment with IL-6. Cells transfected with nonspecific siRNA (NSsiRNA) (SI03650325; Qiagen) were used as controls. 20 min of IL-6 treatment was done to study protein phosphorylation, and treatment for 24 h was performed to study mRNA expression.

Administration of STAT3 Inhibitor (S31-201) and STAT3 siRNA to Renal Artery-ligated Rats—STAT3 inhibitor (S31-201) was administered intraperitoneally in renal artery-ligated rats at a dose of 5 mg/kg of body weight from the 1st day of ligation until the 14th day (30). A separate group of renal artery-ligated animals (vehicle group) was also injected with an equivalent concentration of the solvent (DMSO) in which S31-201 was dissolved. STAT3 siRNA for *in vivo* delivery (*In vivo* Direct siRNA; s129047; Ambion) was dissolved in RNase free 1× sterile PBS and was directly injected to the ventricles of ligated animals ($n = 10$) following the manufacturer's instructions at a concentration of 10 nmol from the 1st day of ligation until the 14th day (22). Another group of renal artery-ligated rats was also treated with nonspecific control siRNA (NSsiRNA) (4404020; Ambion). After 14 days animals were sacrificed, and heart tissues were collected in liquid N_2 and stored in −80 °C for future use.

Statistical Analysis—All results are expressed as ±S.E. Data were analyzed with one way analysis of variance followed by Student's t test using SPSS software (Version 14.0). Experiments were repeated at least three times before analysis. Results with p value <0.05 were considered significant.

RESULTS

Estimation of Circulating IL-6 Level during Hypertrophy—The role of IL-6 in hypertrophy has been reported by several authors (8–11). To confirm release of IL-6 during renal artery ligation-induced hypertrophy, serum IL-6 was measured by ELISA. A significant increase in the circulating IL-6 level was observed in the serum of renal artery-ligated rats (721.416 ± 34.45 pg/ml) compared with sham-operated control animals (39.33 ± 12.96 pg/ml; Fig. 1*A*). Treatment of renal artery-ligated animals with neutralizing IL-6 antibody showed a 48.1% decrease in circulating IL-6 level compared with ligated rats (Fig. 1*A*). Western blotting also showed a significant decrease in IL-6 levels in rat ventricular tissue after IL-6 neutralization (data not shown) together with a significant decrease in expression of hypertrophy marker genes as revealed by RT-PCR (Fig. 1*B*), suggesting that increased circulating IL-6 after renal artery ligation was responsible for development of cardiac hypertrophy in rats.

Isolated cardiac fibroblasts treated with IL-6 or AngII was used to generate hypertrophy *in vitro*. Cultured cardiac fibroblasts were treated with 10^{-8} mol/liter (Sar^1)-Angiotensin II with or without neutralizing IL-6 antibody, and secreted IL-6 levels in culture supernatant were estimated by ELISA. A significant increase in secreted IL-6 levels was observed in supernatants of AngII-treated fibroblasts (283.5 ± 38.21 pg/ml) compared with untreated control cells (127.25 ± 11.59 pg/ml), which was reduced significantly when IL-6 was preincubated with neutralizing IL-6 antibody before treatment (data not shown).

Up-regulation of Collagen Expression during Hypertrophy—A significant increase in collagen expression was observed in the ventricular tissue of renal artery-ligated rats (Fig. 1*C*). The role of IL-6 in the collagen induction process in our renal artery-ligated rats was confirmed by treating the ligated rats with neutralizing IL-6 antibody, which showed a significant decrease (29.72%) in total ventricular collagen content (Fig. 1*C*). Similarly, IL-6 neutralization *in vitro* also resulted in significant decrease (48.24%) in IL-6-induced collagen expression in cultured cardiac fibroblast cells (Fig. 1*D*).

Phosphorylation of STAT and MAPK Proteins during Hypertrophy—Time-dependent phosphorylation of STAT1 (Tyr-701 and Ser-727), STAT3 (Tyr-705 and Ser-727), p38 MAPK, and ERK1/2 was observed after IL-6 treatment of cultured cardiac fibroblasts. Maximum phosphorylation of all these signaling proteins was observed within 15–30 min of IL-6 treatment (supplemental Figs. 1*A* and 2*A*). Earlier results were corroborated by an immunofluorescence study where IL-6-treated (20 min) cardiac fibroblasts showed induction and nuclear translocation of p-STAT1-Tyr-701, p-STAT3-Tyr-705, p-p38 MAPK, and p-ERK1/2 proteins compared with untreated cells (supplemental Figs. 1, *B* and *C*, and 2, *B* and *C*). Cells were counterstained with anti-vimentin antibody (green fluorescence) for fibroblasts specificity. A similar time-dependent phosphorylation of these proteins was observed in AngII-treated cardiac fibroblasts (data not shown).

To block the phosphorylation of these proteins, cultured cardiac fibroblasts were pretreated with specific inhibitors to these

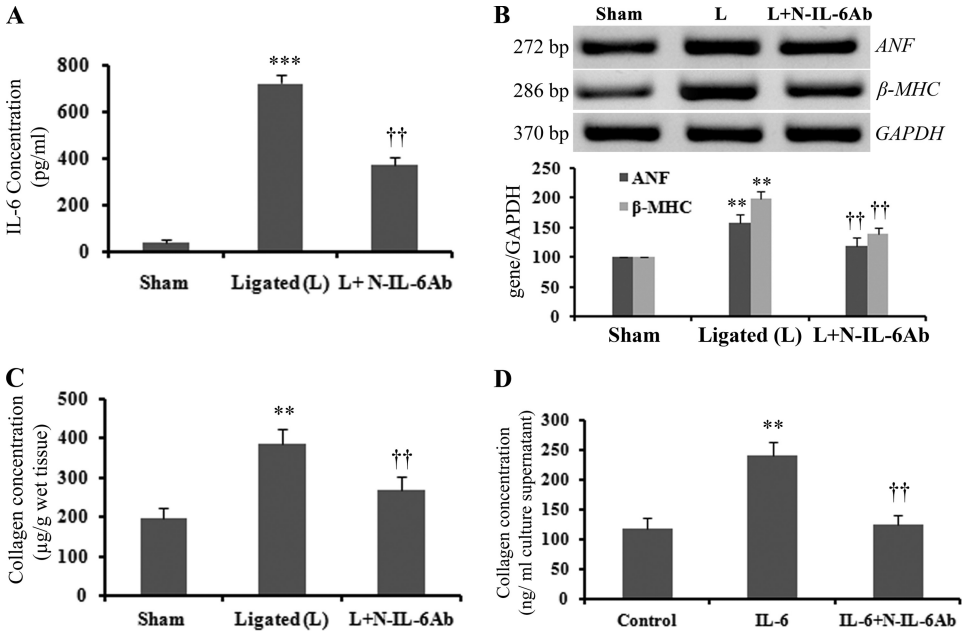

FIGURE 1. **IL-6-induced collagen synthesis during hypertrophy *in vivo* and *in vitro*.** *A*, serum IL-6 concentration was measured by ELISA on day 15 after renal artery ligation in rats, and results show a significant increase in secreted IL-6 level in the serum of renal artery-ligated (*L*) animals (721.42 ± 34.45 pg/ml) compared to sham-operated controls (39.33 ± 12.96 pg/ml), which was reduced significantly (48.1%) with neutralizing IL-6 antibody (*L+N-IL-6Ab*) treatment (10 μg/animal; on alternate days after renal artery ligation till sacrifice). Results are expressed as the ±S.E. of three independent experiments. **, $p < 0.01$ with respect to Sham; ††, $p < 0.01$ with respect to ligated; $n = 10$ in each group. *B*, RT-PCR shows induction of hypertrophy marker genes *ANF* and *β-MHC* in renal artery-ligated rats (*second lane*, *L*) compared to sham-operated controls (*first lane*, *Sham*). Animals were sacrificed on day 15 after surgery. Neutralizing IL-6 antibody treatment caused a significant reduction in *ANF* (25%) and *β-MHC* (29.9%) gene expression in renal artery-ligated animals (*third lane*, *L+N-IL-6Ab*). *GAPDH* was used as the loading control. Representative graph showing induction of *ANF* and *β-MHC* gene expression in renal artery-ligated rats and down-regulation upon neutralizing IL-6 antibody treatment. *C*, hydroxyproline assay shows a significant increase in total ventricular collagen content in renal artery-ligated animals (383.79 ± 40.9 μg/g) compared to sham animals (195.64 ± 28.23 μg/g). Ventricular collagen concentration was reduced significantly (29.72%) upon neutralizing IL-6 treatment to renal artery-ligated rats. Results are expressed as ±S.E. of three independent experiments. **, $p < 0.01$ with respect to Sham; ††, $p < 0.01$ with respect to Ligated; $n = 10$ in each group. Experiments were done on day 15th after surgery. *D*, IL-6 treatment (24 h) in cultured cardiac fibroblasts showed a significant increase in secreted collagen concentration in fibroblast culture supernatant (240.88 ± 23.33 ng/ml) compared to untreated controls (118.52 ± 19.66 ng/ml), which was again reduced significantly (48.24%) when IL-6 was preincubated with neutralizing IL-6 antibody before treatment for 1 h. Results are expressed as ±S.E. of three independent experiments. **, $p < 0.01$ with respect to control; ††, $p < 0.01$ with respect to IL-6 treatment.

proteins before IL-6 treatment. Because maximum activation of STAT3, STAT1, ERK, and p38 MAPK proteins was achieved within 20 min, IL-6 treatment was done for 20 min to check phosphorylation status after inhibitor treatment (supplemental Figs. 1*A* and 2*A*). Western blotting results showed that p-STAT3-Tyr-705 level was decreased by 2.6 ± 0.2-fold ($p < 0.01$) in the presence of STAT3 inhibitor S31-201 (Fig. 2*A*; supplemental Fig. 3*A*). No significant change in p-STAT3-Ser-727 and total STAT3 level was observed (Fig. 2*A*; supplemental Fig. 3*A*). Fludarabine (STAT1 inhibitor) decreased phosphorylation of STAT1 at Tyr-701 by 2 ± 0.15-fold ($p < 0.01$). No change was observed in p-STAT1-Ser-727 and total STAT1 level upon inhibitor treatment (Fig. 2*B*; supplemental Fig. 3*B*). SB203580 (p38 MAPK inhibitor) and U0126 (ERK1/2 inhibitor) also decreased phosphorylation of the respective proteins by 2.5 ± 0.18-fold ($p < 0.01$) and 1.6 ± 0.23-fold ($p < 0.01$), respectively (Fig. 2*B*; supplemental Fig. 3, *C* and *D*). No change was observed in total p38 MAPK and ERK1/2 levels after inhibitor treatment (Fig. 2*B*).

Inhibition of STAT3 and p38 MAPK Resulted in Regression of Collagen Gene Expression in Fibroblasts Stimulated by IL-6—Collagen up-regulation was estimated in IL-6 (50 ng/ml)-treated cultured cardiac fibroblasts by real time PCR. An 1.82 ± 0.12-fold ($p < 0.001$) and 1.69 ± 0.15-fold ($p < 0.001$) increase in *collagen 1*, *collagen 3* gene expression, respectively, was observed in IL-6-treated fibroblasts (Fig. 2*C*). A significant increase (~2-fold) in total secreted collagen in IL-6-treated fibroblast culture supernatant (240.88 ± 23.33 ng/ml) was also observed as compared to untreated supernatant (118.52 ± 19.66 ng/ml; Fig. 2*D*). To confirm whether activation of STAT3, STAT1, p38 MAPK, or ERK1/2 by IL-6 has any significant role in collagen synthesis, inhibitors to these proteins were used to block their activation before IL-6 treatment, and collagen expression was studied. Inhibition of STAT3 phosphorylation by S31-201 resulted in significant down-regulation of IL-6-induced *collagen 1* (1.47 ± 0.1-fold; $p < 0.001$) and *collagen 3* gene expression (1.4 ± 0.12-fold; $p < 0.001$) in cultured fibroblasts (Fig. 2*C*). STAT3 inhibitor also significantly reduced total secreted collagen content in the culture supernatant of inhibitor-treated fibroblasts compared to only IL-6-treated culture supernatant (135.67 ± 19.32 ng/ml *versus* 240.88 ± 23.33 ng/ml, *i.e.* 43.68 ± 2.6% regression; Fig. 2*D*). However, STAT1 inhibitor, fludarabine, did not show any significant down-regulation of either *collagen 1* or *collagen 3* expression and total secreted collagen content compared to IL-6-treated fibroblasts (Fig. 2, *C* and *D*).

Collagen 1 (1.14 ± 0.08-fold; $p < 0.05$) and *collagen 3* (1.1 ± 0.06-fold; $p < 0.05$) expression was also significantly regressed by p38 MAPK inhibitor SB203580 *in vitro* (Fig. 2*C*). In the presence of SB203580, total secreted collagen content in culture

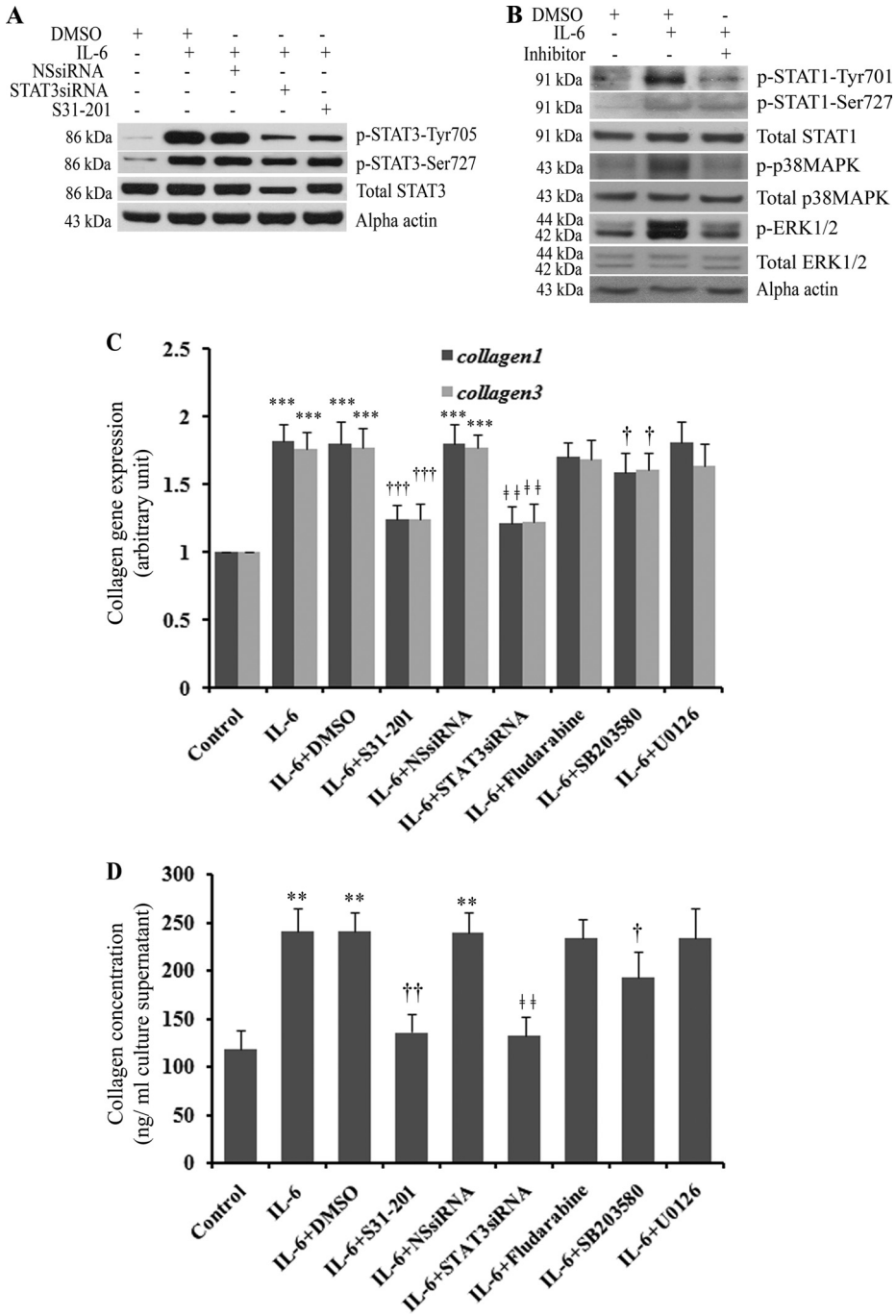

FIGURE 2. *A*, Western blotting results show phosphorylation of STAT3 (Tyr-705/Ser-727) upon treatment of cultured cardiac fibroblasts with IL-6 for 20 min (*second lane*, *IL-6+DMSO*; *third lane*, *IL-6+NSsiRNA*). p-STAT3-Tyr-705 level was reduced significantly with STAT3-specific siRNA (*fourth lane*, *IL-6+STAT3 siRNA*) as well as STAT3 inhibitor S31-201 (*fifth lane*, *IL-6+S31-201*) treatment together with IL-6. The p-STAT3-Ser-727 level was also reduced by 1.3 ± 0.14-fold ($p < 0.05$) upon siRNA treatment. Although, S31-201 treatment did not change the total STAT3 level, siRNA treatment resulted in a 1.52 ± 0.2-fold ($p < 0.01$) decrease in total STAT3 level. α-Actin was used as the internal loading control. *B*, Western blotting results show phosphorylation (*second lane*) of p38 MAPK, ERK1/2, and STAT1 (Tyr-701 and Ser-727) in cultured cardiac fibroblasts upon IL-6 treatment (20 min) that were significantly reduced (*third lane*) by treatment with specific inhibitors for STAT1 (fludarabine, 50 μM), p38 MAPK (SB203580, 10 μM), and ERK1/2 (U0126, 10 μM). No significant change in p-STAT-Ser-727 level was observed upon fludarabine treatment. Total STAT1, p38 MAPK, and ERK1/2 proteins were unchanged during the treatment. *C*, down-regulation of collagen gene expression with STAT3 and p38 MAPK inhibitors is shown. Significant down-regulation of *collagen 1* (1.47-fold, $p < 0.001$) and *collagen 3* transcripts (1.4-fold, $p < 0.001$) was observed in IL-6-induced (24 h) fibroblasts and treated with STAT3 inhibitor S31-201 as shown by real time PCR. Both *collagen 1* and *3* gene expressions were also decreased significantly (1.5- and 1.39-fold, respectively; $p < 0.01$) with STAT3 siRNA treatment in IL-6-induced cardiac fibroblasts. Fludarabine (STAT1 inhibitor) and U0126 (ERK1/2 inhibitor) had no effect on collagen gene expression. SB203580 treatment resulted in down-regulation of both *collagen 1* (1.14-fold, $p < 0.05$) and *collagen 3* transcript (1.1-fold, $p < 0.05$) levels in IL-6-treated fibroblasts. Results are expressed as ±S.E. of three independent experiments. ***, $p < 0.001$ with respect to control; †††, $p < 0.001$ and †, $p < 0.05$ with respect to IL-6+DMSO treatment; ‡‡, $p < 0.01$ with respect to IL-6+NSsiRNA treatment). *D*, hydroxyproline assay shows a 43.68 and 44.9% decrease in IL-6-induced (24 h) collagen synthesis in cultured fibroblasts using S31-201 and STAT3 siRNA, respectively. STAT1and ERK1/2 inhibitors had no effect on IL-6-induced collagen synthesis. p38 MAPK inhibition also resulted in significant regression of total secreted collagen (19.71% regression) in IL-6-induced fibroblast supernatants. Results are expressed as ±S.E. of three independent experiments. **, $p < 0.01$ with respect to control; ††, $p < 0.01$ and †, $p < 0.05$ with respect to IL-6+DMSO treatment; ‡‡, $p < 0.01$ with respect to IL-6+NSsiRNA treatment.

supernatant was also significantly lower in IL-6-treated fibroblasts (19.71 ± 1.3%, regression) compared to IL-6-treated cells without inhibitor (Fig. 2*D*), although the down-regulation of collagen synthesis was less pronounced compared to STAT3 inhibitor. ERK1/2 inhibitor (U0126) had no significant effect on either collagen transcripts or protein expression in IL-6-treated fibroblasts (Fig. 2, *C* and *D*). At doses used in this study, <10% cell mortality was observed in fibroblasts after 24 h of treatment, as estimated by an MTS (3-(4,5-dimethylthiazol-2-yl)-5-(3-carboxymethoxyphenyl)-2-(4-sulfophenyl)-2H-tetrazolium) assay (data not shown).

Since STAT3 inhibitor treatment resulted in maximum down-regulation of IL-6-induced collagen synthesis, the role of STAT3 in collagen induction process was reconfirmed by using STAT3-specific siRNA in cultured fibroblasts. The effect of siRNA treatment on STAT3 phosphorylation in IL-6-induced fibroblasts was checked by Western blotting, which showed a 3.6 ± 0.26-fold ($p < 0.01$) reduction in p-STAT3-Tyr-705 level together with a comparatively less pronounced change in p-STAT3-Ser-727 (1.3 ± 0.14-fold; $p < 0.05$) and total STAT3 (1.52 ± 0.2-fold; $p < 0.01$) level (Fig. 2*A*; supplemental Fig. 3*A*). STAT3 siRNA treatment also resulted in 1.5 ± 0.1-fold ($p < 0.01$) and 1.39 ± 0.13-fold ($p < 0.01$) down-regulation in *collagen 1* and *collagen 3* gene expression, respectively, upon IL-6 treatment (Fig. 2*C*). Significant reduction (44.9 ± 3.1% reduction) in total secreted collagen content was also observed with STAT3 siRNA treatment of IL-6-treated cells. No reduction in collagen content was observed with nonspecific siRNA treatment compared with IL-6-treated cells (Fig. 2*D*).

Inhibition of STAT3 Activation in Vivo in Renal Artery-ligated Rats Resulted in Decreased Cardiac Collagen Synthesis—Concurrent to *in vitro* results, significant phosphorylation of STAT3 at Tyr-705 (4.69 ± 0.21-fold; $p < 0.001$) as well as Ser-727 (3.25 ± 0.18-fold; $p < 0.001$) was observed in hypertrophied rat hearts compared to sham-operated animals (Fig. 3, *A* and *B*), with no change in total STAT3 levels. Phosphorylation of STAT1 (Tyr-701 and Ser-727), p38 MAPK, and ERK1/2 was also significantly pronounced in renal artery-ligated rat hearts compared to sham-operated controls (data not shown). To block phosphorylation of STAT3 *in vivo*, renal artery-ligated animals were treated with either S31-201 or STAT3 siRNA, as described under "Experimental Procedures." Western blotting with whole cell extracts prepared from these ventricular tissues showed significant down-regulation in p-STAT3-Tyr-705 levels in STAT3 siRNA as well as S31-201-treated samples (2.9 ± 0.15-fold and 2.6 ± 0.14-fold; $p < 0.01$ respectively) compared to ligated animals treated either with DMSO or nonspecific siRNA (Fig. 3, *A* and *B*). Although, S31-201 treatment did not change p-STAT3-Ser-727 or total STAT3 levels, STAT3 siRNA-treated renal artery-ligated rats showed a decrease in p-STAT3-Ser-727 and total STAT3 levels compared to DMSO or nonspecific siRNA-treated ligated rats (Fig. 3, *A* and *B*). Thus, the efficacy of STAT3 siRNA in down-regulation of STAT3 protein *in vivo* was confirmed.

A significant increase in expression of both *collagen 1* (3.6 ± 0.18-fold; $p < 0.01$) and *collagen 3* (2.9 ± 0.2-fold; $p < 0.01$) genes was also observed *in vivo* in hypertrophied rat hearts compared to sham-operated controls (Fig. 3, *C* and *D*). A significant increase in total collagen content was also observed in ligated heart tissues compared to sham-operated animals (383.79 ± 40.9 μg/g wet tissue *versus* 195.64 ± 28.232 μg/g wet tissue, $p < 0.01$) as revealed by hydroxyproline assay (Fig. 3*E*). Masson's Trichrome staining of ventricular tissue sections revealed substantial infiltration and deposition of collagen in renal artery-ligated rats compared with control tissue sections. Quantitative analysis of the Masson's Trichrome-stained tissue sections revealed that collagen volume fraction (%) in ligated tissue was significantly higher than that of sham-operated animals (20.38 ± 0.99 *versus* 9.42 ± 0.62; $p < 0.001$; data not shown).

Because STAT3 inhibitor treatment *in vitro* showed maximum down-regulation of collagen, *in vivo* experiments were done to confirm the role of STAT3 in collagen biosynthesis process. S31-201 and STAT3 siRNA-treated renal artery-ligated animals showed a significant decrease in both *collagen 1* (2.3 ± 0.2-fold; $p < 0.01$) and *collagen 3* (2.2 ± 0.14-fold; $p < 0.01$) gene expression compared to renal artery-ligated rats with DMSO or nonspecific siRNA treatment (Fig. 3, *C* and *D*). In addition, significant lowering of total ventricular collagen content was also observed in both STAT3 siRNA as well as S31-201-treated animals compared to ligated ones (213.6 ± 29.87 and 222.8 ± 26.1 μg/g, respectively *versus* 383.79 ± 40.9 μg/g wet tissue; $p < 0.01$; Fig. 3*E*). *In vivo* treatment with p38 MAPK inhibitor (SB203580) had no significant effect on collagen gene expression (data not shown).

STAT3 Inhibitor Regulates Expression of Collagen Modulators during Hypertrophy—The expression of MMPs and TIMPs, which are responsible for maintaining homeostatic balance between collagen synthesis and degradation in heart, was analyzed in both *in vitro* as well as *in vivo* hypertrophy models. RT-PCR analysis showed a significant increase in *TIMP-1* (1.76 ± 0.12-fold; $p < 0.01$) and *LOX* (2.27 ± 0.2-fold; $p < 0.01$) transcript levels in IL-6-treated cardiac fibroblasts, but no change was observed for *MMP-2*, *MMP-9*, or *TIMP-2* transcript levels (data not shown). On the contrary, a significant increase in expression of *MMP-2* (1.8 ± 0.2-fold; $p < 0.01$), *MMP-9* (1.6 ± 0.1-fold; $p < 0.001$), *TIMP-1* (1.9 ± 0.2-fold; $p < 0.001$), *TIMP-2* (2.8 ± 0.2-fold; $p < 0.001$), and *LOX* (1.9 ± 0.16-fold; $p < 0.001$) was observed *in vivo* in renal artery-ligated rat hearts compared to sham-operated controls by RT-PCR analysis (Fig. 4, *A* and *B*). Interestingly, increased expression of these collagen regulator genes was significantly down-regulated in hypertrophied rats when treated with STAT3 inhibitor S31-201 as well as STAT3 siRNA (*MMP-2* by 1.45 ± 0.15-fold, $p < 0.01$; *MMP-9* by 2.0 ± 0.1-fold, $p < 0.01$; *TIMP-1* by 1.4 ± 0.11-fold, $p < 0.01$; *TIMP-2* by 1.70 ± 0.16-fold, $p < 0.01$; *LOX* by 1.59 ± 0.15-fold, $p < 0.01$; Fig. 4, *A* and *B*).

Inhibition of STAT3 Activation Resulted in Regression of Cardiac Hypertrophy in Vivo—Previous results confirmed that STAT3 inhibition resulted in down-regulation of collagen biosynthesis. However, whether this had a downstream effect on cardiac hypertrophy process, HW/BW ratio and expression of hypertrophy marker genes were measured. S31-201 and STAT3 siRNA treatment of ligated rats resulted in a significant decrease in HW to BW ratio in these animals (3.15 ± 0.077 and 3.07 ± 0.21, respectively, *versus* 4.03 ± 0.098, $p < 0.001$; Fig.

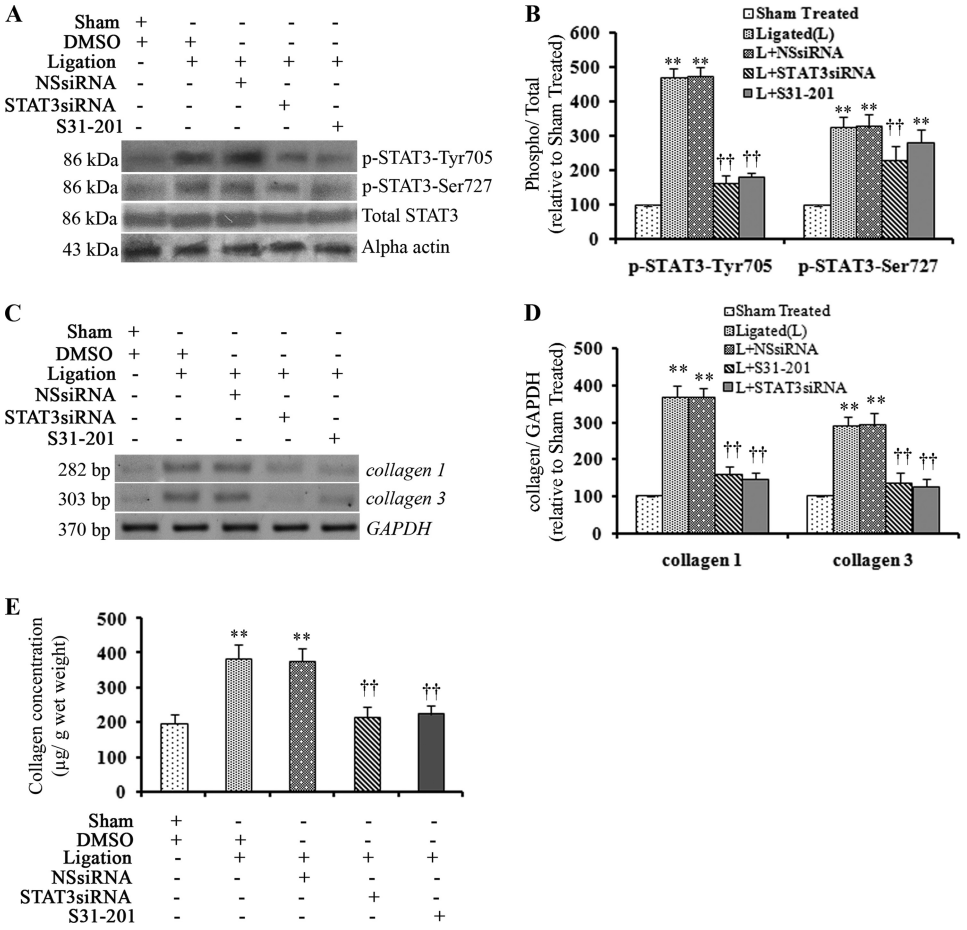

FIGURE 3. ***In vivo* treatment with STAT3 inhibitors reduced cardiac fibrosis in renal artery-ligated rat hearts.** *A*, Western blotting results show increased levels of p-STAT3 (Tyr-705 and Ser-727) in ventricular tissue of renal artery-ligated rats (*second lane* (*Ligation +DMSO*) and *third lane* (*Ligation +*NSsiRNA)). A significant decrease in p-STAT3-Tyr-705 level was observed with STAT3 siRNA (*fourth lane*, *Ligation +STAT3siRNA*) and S31-201 (*fifth lane*, *Ligation +S31-201*) treatment (14 days) to renal artery-ligated rats (2.9- and 2.6-fold respectively. **, $p < 0.01$ with respect to ligated rats treated with DMSO or NSsiRNA. No significant change in p-STAT3-Ser-727 and total STAT3 levels was observed with S31-201 treatment (*fifth lane*). However, STAT3 siRNA treatment showed a significant decrease in p-STAT3-Ser-727 (1.43 ± 0.12; $p < 0.01$; *fourth lane*) and total STAT3 (1.62 ± 0.17-fold; $p < 0.05$; *fourth lane*) levels. α-Actin was used as the internal loading control. *B*, shown is a representative graph of the above Western blots. **, $p < 0.01$ with respect to Sham-treated; ††, $p < 0.01$ with respect to ligated (L) or L+NSsiRNA treatment; $n = 10$ in each group. *C*, RT-PCR showing significantly increased expression of both *collagen 1* and *collagen 3* transcripts (*second lane* (*L+DMSO*) and *third lane* (*Ligation+NSsiRNA*)) in renal artery-ligated rat ventricle. Collagen up-regulation decreased significantly with STAT3 siRNA (*fourth lane*, *Ligation+STAT3siRNA*) and S31-201 (*fifth lane*, *Ligation+S31-201*) treatment (14 days) compared with ligated samples treated with DMSO or NSsiRNA. *GAPDH* was used as the internal loading control. *D*, shown is a graphic representation of the above RT-PCR results. **, $p < 0.01$ with respect to Sham-treated; ††, $p < 0.01$ with respect to ligated (L) or L+NSsiRNA treatment; $n = 10$ in each group. *E*, a significant increase in total ventricular collagen was observed in renal artery-ligated rats as revealed by hydroxyproline assay. Total ventricular collagen was decreased significantly in STAT3 siRNA (213.6 ± 29.87 μg/g wet tissue) as well as S31-201 (222.8 ± 26.1 μg/g wet tissue)- treated ligated rats compared with only ligated animals (383.79 ± 40.9 μg/g wet tissue). Results are expressed as ±S.E. of three independent experiments. **, $p < 0.01$ with respect to Sham-treated; ††, $p < 0.01$ with respect to L or L+NSsiRNA treatment; $n = 10$ in each group).

5*A*). Decreased expression of hypertrophy marker genes *ANF* (1.26 ± 0.1-fold; $p < 0.01$ and 1.29 ± 0.1-fold; $p < 0.01$) and *β-MHC* (1.49 ± 0.15-fold; $p < 0.01$ and 1.54 ± 0.14-fold; $p < 0.01$) and proto-oncogenes c-*jun* (1.4-fold ±0.12; $p < 0.01$ and 1.59 ± 0.1-fold; $p < 0.05$), c-*fos* (1.35 ± 0.12-fold; $p < 0.01$ and 1.41 ± 0.15-fold; $p < 0.01$), and c-*myc* (1.42 ± 0.16-fold; $p < 0.01$ and 1.52 ± 0.15-fold; $p < 0.01$) was also observed in STAT3 siRNA and S31-201-treated hearts, respectively, compared to controls treated with either DMSO or nonspecific siRNA (Fig. 5, *B* and *C*). Inhibition of STAT3 also resulted in significantly improved cardiac function in these renal artery-ligated animals as evident by decreased left ventricular diastolic dimensions and increased fractional shortening % as observed by M-mode echocardiography analysis (Table 1).

DISCUSSION

Cardiac fibrosis leading to ventricular stiffness is responsible for the development of diverse pathological states including cardiac dysfunction during various heart diseases, and accumulation of major extracellular matrix protein collagen 1 is one of the main events in cardiac remodeling process in diseased hearts (31). Increased deposition of collagen proteins was observed in hypertensive heart disease and in patients with dilated cardiomyopathy and end stage heart failure (31). Significant up-regulation of collagen 1 and collagen 3 expression as well as excess collagen deposition was evident in our *in vivo* pressure overload hypertrophy model (Figs. 1*C* and 3, *C–E*). Many growth factors and cytokines have been shown to modulate cardiac hypertrophy and collagen synthesis involving var-

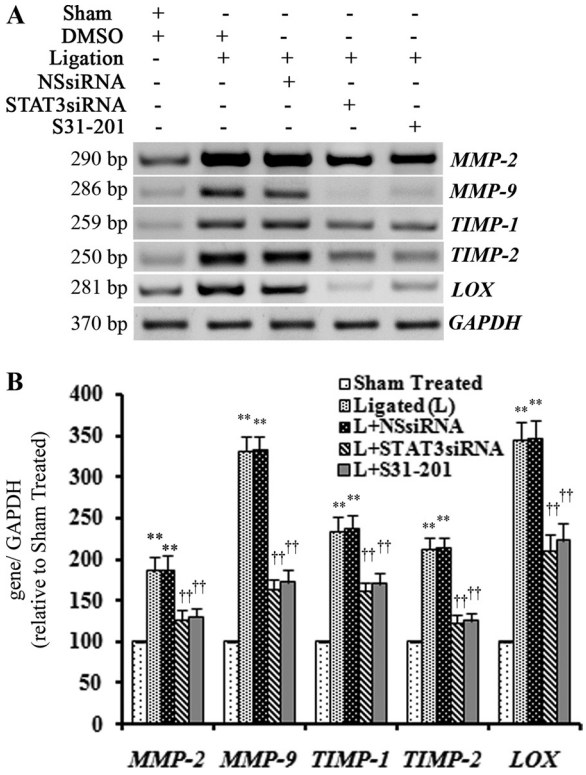

FIGURE 4. ***In vivo* STAT3 inhibition showed decreased expression of collagen modulator genes.** *A*, in renal artery-ligated rats (14 days) expression of collagen modulator genes like *MMP-2*, *MMP-9*, *TIMP-1*, *TIMP-2*, and *LOX* was significantly higher (*second lane* (*Ligation*+*DMSO*) and *third lane* (*Ligation*+*NSsiRNA*)) compared to sham-treated rats (*lane* 1) as revealed by RT-PCR. Significant down-regulation in the expression of collagen modulator genes was observed in STAT3 siRNA (*fourth lane*, *Ligation*+*STAT3siRNA*) and S31-201 (*fifth lane*, *Ligation*+*S31-201*)-treated renal artery-ligated rats compared to untreated hypertrophied rats. *GAPDH* was used as loading control for these experiments. *B*, graphic representation of the above RT-PCR results shows significant down-regulation of *MMP-2*, *MMP-9*, *TIMP-1*, *TIMP-2*, and *LOX* gene expression with STAT3 siRNA and S31-201 treatments (14 days) compared with ligated animals; **, $p < 0.01$ with respect to Sham-treated; ††, $p < 0.01$ with respect to ligated (L) or L+NSsiRNA treatment; $n = 10$ in each group).

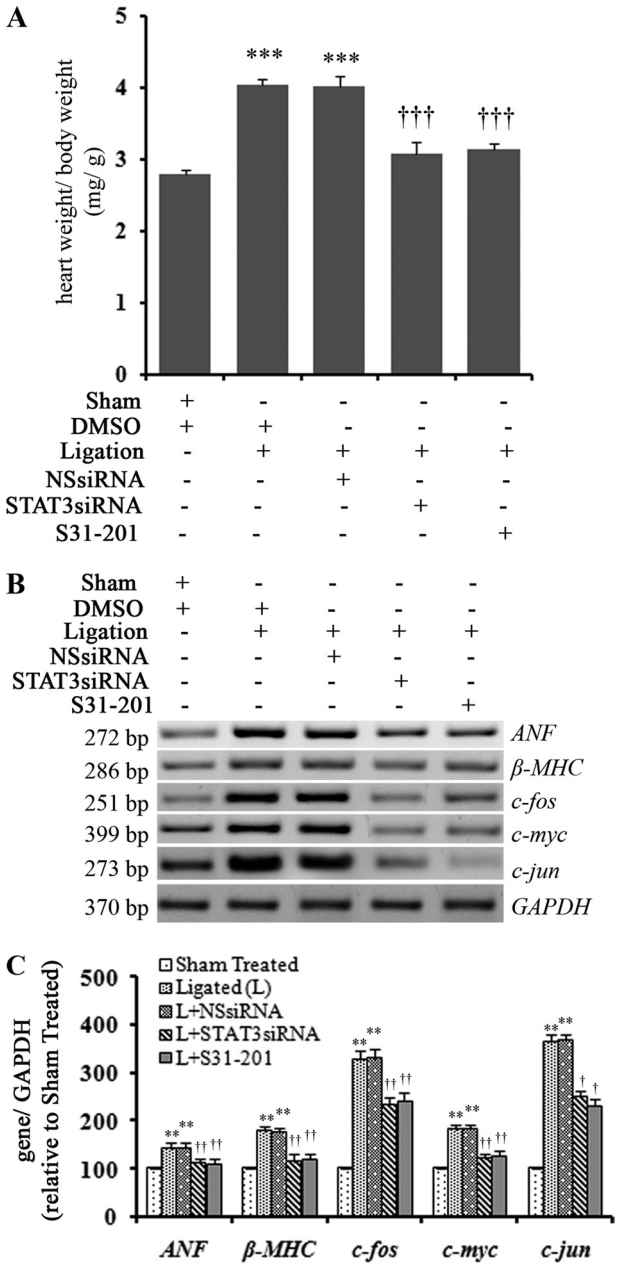

FIGURE 5. ***In vivo* STAT3 inhibition resulted in regression of cardiac hypertrophy.** *A*, the graph shows a significant decrease in HW to BW ratio of STAT3 siRNA (3.07 ± 0.21) as well as S31-201-treated (14 days) ligated animals (3.15 ± 0.077) compared to only ligated animals (4.03 ± 0.098). ***, $p < 0.001$ with respect to Sham-treated; †††, $p < 0.01$ with respect to ligation or ligation+NSsiRNA treatment; $n = 10$ in each group. *B*, RT-PCR results show both STAT3 siRNA (*fourth lane*, ligation+STAT3siRNA) and S31-201(*fifth lane*, ligation+S31-201) treatment (14 days), resulting in significant down-regulation of hypertrophy marker genes (*ANF* and *β-MHC*) and proto-oncogenes (c-*jun*, c-*fos*, and c-*myc*) expression in renal artery-ligated (*L*) animals compared to DMSO or NSsiRNA treated renal artery-ligated rats (*second lane* (*Ligation*+*DMSO*) and *third lane* (*Ligation*+*NSsiRNA*)). *GAPDH* was used as internal loading control. *C*, a graphic representation of RT-PCR data shows down-regulation of *ANF*, *β-MHC*, c-*jun*, c-*fos*, and c-*myc* gene expression with S31-201 and STAT3 siRNA treatments respectively compared to ligated animals. **, $p < 0.01$ with respect to Sham-treated; ††, $p < 0.01$ and †, $p < 0.05$ with respect to ligated (L) or L+NSsiRNA treatment; $n = 10$ in each group).

ious signaling pathways in isolated systems (3). Increased activity of IL-6, a proinflammatory cytokine during hypertrophy and heart failure has been reported by several authors (32). Melén-dez *et al.* (11) showed that IL-6 infusion causes left ventricular hypertrophy and myocardial fibrosis in rats. AngII, known to induce cardiac hypertrophy involving renin-angiotensin system, was shown to induce IL-6 production both in cultured cardiac fibroblasts and during maladaptive pressure overload hypertrophy via activation of gp130 (9, 10, 13). IL-6 has been shown to increase collagen synthesis both in *in vitro* cultured fibroblasts and in *in vivo* rat hearts (8, 9, 11). Consistent with these previous studies, we also observed increased levels of IL-6 after AngII treatment of cardiac fibroblasts (data not shown) as well as up-regulation of collagen expression by IL-6 (Figs. 1*D* and 2, *C* and *D*). Despite its significant role, precise mechanism of IL-6-induced hypertrophy has not yet been clearly understood. In this study we have tried to look into the involvement of various signaling molecules associated with IL-6-mediated fibrosis and eventual compromised cardiac function. To confirm the role of IL-6 during hypertrophy, neutralizing IL-6 antibody was administered to the renal artery-ligated animals to neutralize the serum IL-6. IL-6 neutralization partially reduced cardiac hypertrophy as well as collagen synthesis in rat heart (Fig. 1, *B* and *C*). Total regression of hypertrophy after IL-6

TABLE 1
M-mode echocardiography data
LVDD, left ventricular diastolic dimensions; FS, fractional shortening; NS, significant.

	LVDD	FS	*p* value
	mm	%	
Sham-operated	0.45 ± 0.02	61 ± 3.7	NS
Renal artery-ligated (Ligated)	0.54 ± 0.04	43 ± 2.5	$p < 0.05$ *vs.* sham
Ligated + DMSO	0.55 ± 0.05	41 ± 2.6	NS *vs.* ligated
Ligated + S31-201	0.47 ± 0.01	54 ± 2.9	$p < 0.05$ *vs.* ligated + DMSO
Ligated + nonspecific siRNA	0.53 ± 0.06	42 ± 2.8	NS *vs.* ligated
Ligated + STAT3siRNA	0.46 ± 0.02	55.6 ± 3.2	$p < 0.05$ *vs.* ligated + nonspecific siRNA

neutralization did not occur, as several other factors also play a role during cardiac hypertrophy *in vivo* (33).

Downstream signaling by IL-6-gp130 axis involves activation of two major signaling pathways, namely JAK-STAT and MAPK-ERK; thus, significance of both pathways during hypertrophy was analyzed. Previous studies have shown increased tyrosine phosphorylation of STAT1 and STAT3 proteins during cardiac hypertrophy. Activation of STAT1 and STAT3 in the heart plays a very significant role in cardiac pathophysiology during various diseases, and their activity is increased during mechanical overload (34). During this study too, time-dependent phosphorylation of both STAT1 and STAT3 at tyrosine as well as serine residues in IL-6-stimulated cultured cardiac fibroblasts was observed (supplemental Fig. 1, *A–C*). Serine phosphorylation of both STATs achieved a maximum level before Tyr phosphorylation, which is suggestive of their role in regulation of full transcriptional activity of STAT proteins.

Although, total STAT3 deletion leads to embryonic lethality, cardiac-specific STAT3 deletion causes increased infarct size after ischemia/reperfusion injury (35, 36). STAT3 overexpression results in decreased infarct size induced by ischemia/reperfusion injury and gives protection to cardiac myocytes during hypoxia/reoxygenation induced cell loss (37, 38). Heart failure patients with end stage-dilated cardiomyopathy shows increased tyrosine phosphorylation of STAT3, but it is also established that STAT3 activation is instrumental in inhibition of apoptosis and necessary to promote compensatory hypertrophy and thus helps in prevention of heart failure (39). During ischemia, STAT3 protects the myocardium against STAT1-induced apoptosis (40, 41). Although various roles of both these STAT proteins have been illustrated in heart, their involvement in collagen up-regulation and fibrosis process was not described. Primarily it was hypothesized that the calcium channel blocker Mibefradil inhibits AngII or aldosterone-induced cardiac fibrosis, suggesting the role of calcium signaling (42). Tranilast, used to treat allergic manifestations, also attenuated renovascular hypertension and myocardial fibrosis via inhibition of TGF-β signaling (43). AngII-induced cardiac fibrosis in mice was also attenuated through modulation of TGF-β/Smad signaling cascade with allopurinol (44). In addition, angiotensin-converting enzyme inhibitor, ramipril and enalapril, treatment also reverses renal failure-induced left ventricular hypertrophy and fibrosis in rats (45, 46). In our study inhibition of STAT3 phosphorylation with both S31-201 as well as STAT3 siRNA resulted in decreased collagen synthesis by IL-6 in cultured cardiac fibroblasts and also during pressure overload-induced cardiac hypertrophy *in vivo* (Figs. 2, *C* and *D*, and 3, *C–E*). Although STAT1 was activated during this process, it did not have any significant role in collagen induction process (Fig. 2, *C* and *D*). Studies have shown involvement of STAT1 in induction of proapoptotic genes and also development of hypoxic eccentric hypertrophy together with STAT3 (47). STAT1 also has been shown to inhibit endothelial cell migration and tube formation in heart and thus opposes the effect of STAT3 in this respect (48, 49). Further investigation is needed to delineate the role of STAT1 induction during IL-6-induced cardiac hypertrophy.

Similar to JAK-STAT pathways, MAP kinases phosphorylate their target proteins at specific serine/threonine residues to regulate their activity in myocardium (50). Increased activity of p38 MAPK has been observed during pressure overload-induced hypertrophy and in human heart failure (51–53). Inhibition of MAPK signaling has been shown to block hypertrophy both *in vitro* as well as *in vivo* and end organ damage during hypertensive heart disease, suggesting their role in hypertrophic signaling (52, 54). IL-6 has been shown to activate serine/threonine kinases, which includes activation of p38 MAPK and ERK1/2 during cardiac remodeling (32, 33). In addition to activation of p38 MAPK during hypertrophy, its role in the collagen induction process in isolated fibroblasts stimulated by IL-6 was observed in this study. Blocking p38 MAPK phosphorylation using its inhibitor (SB203580), collagen up-regulation was particularly regressed. The effect of p38 MAPK inhibitor was lower (~19%) compared to STAT3 inhibitor (~44% regression; Fig. 2, *C* and *D*) *in vitro*. Although, *in vivo* p38 MAPK inhibition could not regress the collagen induction process in this study, there are reports indicating the role of p38 MAPK signaling in serine phosphorylation of STAT proteins, which could be another possible mechanism by which MAPK affects the collagen induction process during hypertrophy (14, 15, 18). Again, several studies have established the role of ERK1/2 signaling in development of cardiac hypertrophy (55, 56), corroborating our result that has shown prominent ERK1/2 activation *in vitro* (supplemental Fig. 2, *A* and *C*) as well as the *in vivo* (data not shown) model of hypertrophy, but at the same time, ERK1/2 inhibitor had no significant effect on collagen up-regulation process during hypertrophy (Fig. 2, *C* and *D*).

The extracellular collagen degradation is regulated by the ratio of MMPs and TIMPs (6), and their increased expression in failing myocardium has been reported (5). In renal artery-ligated hearts, a significant increase in expression of *MMP-2*, *MMP-9*, *TIMP-1*, and *TIMP-2* was observed (Fig. 4, *A* and *B*). In contrast, only TIMP-1 expression was induced after *in vitro* treatment of cardiac fibroblasts by IL-6. This further confirms that IL-6 alone may result in induction of hypertrophy markers *in vitro*, but other cytokines in addition to IL-6 might play significant role in collagen modulation in renal artery-ligated hypertrophy *in vivo* (33). Compared with MMPs, a pronounced

increase in expression of TIMPs was observed, suggesting lesser degradation and thus increased accumulation of collagen in the myocardium during hypertrophy. In addition, increased LOX expression (Fig. 4, *A* and *B*) further confirms increased collagen turnover during hypertrophy. Moreover, decreased expression of all these genes *in vivo* after treatment with the STAT3 inhibitor and siRNA suggest that activation of STAT3 during hypertrophy directly induces collagen synthesis as well as indirectly regulates collagen modulators to alter their expression to indirectly up-regulate collagen accumulation.

In vivo treatment with STAT3 inhibitor (S31-201) and STAT3 siRNA to the renal artery-ligated rats also resulted in regression of hypertrophy, as evident by a significant decrease in HW to BW ratio along with significant down-regulation in expression of hypertrophy marker genes and proto-oncogenes (Fig. 5, *A–C*). Reversal of hypertrophy after STAT3 inhibition by parthenolide has also recently been shown by Skoumal *et al.* (57), but the mechanism by which STAT3 could modulate hypertrophy process was not defined. Furthermore, it was shown that parthenolide treatment attenuated AngII-induced IL-6 mRNA levels (57), but in our *in vivo* rat model of hypertrophy, STAT3 inhibitors did not show any decrease in circulating IL-6 level (data not shown), suggesting that STAT3 is the downstream signaling molecule in IL-6-mediated collagen synthesis during hypertrophy. Results also suggest that reversal of hypertrophy process by STAT3 inhibition is associated with down-regulation of collagen synthesis although the hypertrophy regression due to STAT3 inhibition was much more pronounced compared with IL-6 neutralization in hypertrophy model *in vivo*. It is possible that during renal artery ligation other than IL-6, other cytokines and growth factors are induced that may also modulate cardiac fibrosis and resultant hypertrophy (33, 58). Regression of cardiac hypertrophy was directly correlated with improved cardiac function in these animals, as shown by M-mode echocardiography data marked by decreased left ventricular diastolic dimensions and significantly increased % fractional shortening (Table 1).

This is the first report on positive role of STAT3 during IL-6-mediated collagen gene up-regulation during hypertrophy. Specific STAT3 inhibition not only down-regulated IL-6-induced collagen synthesis significantly but also effectively regressed the pressure overload-induced cardiac hypertrophy by reducing the fibrosis process. Although, both STAT3 and STAT1 have been implicated to play a role in cardiac hypertrophy, our results suggest that STAT3 and not STAT1 is the major transcription factor that up-regulates myocardial collagen synthesis during hypertrophy, and p38 MAPK activation may have an indirect role by enhancing STAT3 signaling. Thus, STAT3 could be a potential therapeutic target for regulating cardiac fibrosis during myocardial pressure-overload hypertrophy and improvement of cardiac function.

Acknowledgment—We gratefully acknowledge Dr. Mamta Chawla-Sarkar, Department of Virology, National Institute of Cholera and Enteric Diseases, Kolkata, for valuable input during manuscript preparation.

REFERENCES

1. Bishop, J. E., Rhodes, S., Laurent, G. J., Low, R. B., and Stirewalt, W. S. (1994) Increased collagen synthesis and decreased collagen degradation in right ventricular hypertrophy induced by pressure overload. *Cardiovasc. Res.* **28,** 1581–1585
2. Crabos, M., Roth, M., Hahn, A. W., and Erne, P. (1994) Characterization of angiotensin II receptors in cultured adult rat cardiac fibroblasts. Coupling to signaling systems and gene expression. *J. Clin. Invest.* **93,** 2372–2378
3. Kapoun, A. M., Liang, F., O'Young, G., Damm, D. L., Quon, D., White, R. T., Munson, K., Lam, A., Schreiner, G. F., and Protter, A. A. (2004) B-type natriuretic peptide exerts broad functional opposition to transforming growth factor-β in primary human cardiac fibroblasts. Fibrosis, myofibroblast conversion, proliferation, and inflammation. *Circ. Res.* **94,** 453–461
4. Weber, K. T., and Brilla, C. G. (1991) Pathological hypertrophy and cardiac interstitium. Fibrosis and renin-angiotensin-aldosterone system. *Circulation* **83,** 1849–1865
5. Sivakumar, P., Gupta, S., Sarkar, S., and Sen, S. (2008) Up-regulation of lysyl oxidase and MMPs during cardiac remodeling in human dilated cardiomyopathy. *Mol. Cell. Biochem.* **307,** 159–167
6. Siwik, D. A., Chang, D. L., and Colucci, W. S. (2000) Interleukin-1β and tumor necrosis factor-α decrease collagen synthesis and increase matrix metalloproteinase activity in cardiac fibroblasts *in vitro*. *Circ. Res.* **86,** 1259–1265
7. Mäki, J. M., Räsänen, J., Tikkanen, H., Sormunen, R., Mäkikallio, K., Kivirikko, K. I., and Soininen, R. (2002) Inactivation of the lysyl oxidase gene Lox leads to aortic aneurysms, cardiovascular dysfunction, and perinatal death in mice. *Circulation* **106,** 2503–2509
8. Pathak, M., Sarkar, S., Vellaichamy, E., and Sen, S. (2001) Role of myocytes in myocardial collagen production. *Hypertension* **37,** 833–840
9. Sarkar, S., Vellaichamy, E., Young, D., and Sen, S. (2004) Influence of cytokines and growth factors in AngII-mediated collagen up-regulation by fibroblasts in rats. Role of myocytes. *Am. J. Physiol. Heart Circ. Physiol.* **287,** H107–H117
10. Sano, M., Fukuda, K., Kodama, H., Pan, J., Saito, M., Matsuzaki, J., Takahashi, T., Makino, S., Kato, T., and Ogawa, S. (2000) Interleukin-6 family of cytokines mediate angiotensin II-induced cardiac hypertrophy in rodent cardiomyocytes. *J. Biol. Chem.* **275,** 29717–29723
11. Meléndez, G. C., McLarty, J. L., Levick, S. P., Du, Y., Janicki, J. S., and Brower, G. L. (2010) Interleukin-6 mediates myocardial fibrosis, concentric hypertrophy, and diastolic dysfunction in rats. *Hypertension* **56,** 225–231
12. Kurdi, M., and Booz, G. W. (2007) Can the protective actions of JAK-STAT in the heart be exploited therapeutically? Parsing the regulation of interleukin-6-type cytokine signaling. *J. Cardiovasc. Pharmacol.* **50,** 126–141
13. Fischer, P., and Hilfiker-Kleiner, D. (2007) Survival pathways in hypertrophy and heart failure. The gp130-STAT3 axis. *Basic Res. Cardiol.* **102,** 279–297
14. Xu, B., Bhattacharjee, A., Roy, B., Xu, H. M., Anthony, D., Frank, D. A., Feldman, G. M., and Cathcart, M. K. (2003) Interleukin-13 induction of 15-lipoxygenase gene expression requires p38 mitogen-activated protein kinase-mediated serine 727 phosphorylation of Stat1 and Stat3. *Mol. Cell. Biol.* **23,** 3918–3928
15. Ng, D. C., Long, C. S., and Bogoyevitch, M. A. (2001) A role for the extracellular signal-regulated kinase and p38 mitogen-activated protein kinases in interleukin-1β-stimulated delayed signal tranducer and activator of transcription 3 activation, atrial natriuretic factor expression, and cardiac myocyte morphology. *J. Biol. Chem.* **276,** 29490–29498
16. Bolli, R., Dawn, B., and Xuan, Y. T. (2001) Emerging role of the JAK-STAT pathway as a mechanism of protection against ischemia/reperfusion injury. *J. Mol. Cell. Cardiol.* **33,** 1893–1896
17. Mascareno, E., El-Shafei, M., Maulik, N., Sato, M., Guo, Y., Das, D. K., and Siddiqui, M. A. (2001) JAK/STAT signaling is associated with cardiac dysfunction during ischemia and reperfusion. *Circulation* **104,** 325–329
18. Zauberman, A., Zipori, D., Krupsky, M., and Ben-Levy, R. (1999) Stress-activated protein kinase p38 is involved in IL-6-induced transcriptional

activation of STAT3. *Oncogene* **18,** 3886–3893
19. Kunisada, K., Tone, E., Fujio, Y., Matsui, H., Yamauchi-Takihara, K., and Kishimoto, T. (1998) Activation of gp130 transduces hypertrophic signals via STAT3 in cardiac myocytes. *Circulation* **98,** 346–352
20. Barry, S. P., Townsend, P. A., Latchman, D. S., and Stephanou, A. (2007) Role of the JAK-STAT pathway in myocardial injury. *Trends. Mol. Med.* **13,** 82–89
21. Sil, P., and Sen, S. (1997) Angiotensin II and myocyte growth. Role of fibroblasts. *Hypertension* **30,** 209–216
22. Chatterjee, A., Mir, S. A., Dutta, D., Mitra, A., Pathak, K., and Sarkar, S. (2011) Analysis of p53 and NF-κB signaling in modulating the cardiomyocyte fate during hypertrophy. *J. Cell. Physiol.* **226,** 2543–2554
23. Sen, S., Tarazi, R. C., Khairallah, P. A., and Bumpus, F. M. (1974) Cardiac hypertrophy in spontaneously hypertensive rats. *Circ. Res.* **35,** 775–781
24. Wang, G. Y., Sun, B., Kong, Q. F., Zhang, Y., Li, R., Wang, J. H., Wang, D. D., Lv, G. X., and Li, H. L. (2008) IL-17 eliminates the therapeutic effects of myelin basic protein-induced nasal tolerance in experimental autoimmune encephalomyelitis by activating IL-6. *Scand. J. Immunol.* **68,** 589–597
25. Stegemann, H., and Stalder, K. (1967) Determination of hydroxyproline. *Clin. Chim. Acta* **18,** 267–273
26. Sarkar, S., Chawla-Sarkar, M., Young, D., Nishiyama, K., Rayborn, M. E., Hollyfield, J. G., and Sen, S. (2004) Myocardial cell death and regeneration during progression of cardiac hypertrophy to heart failure. *J. Biol. Chem.* **279,** 52630–52642
27. Frias, M. A., Rebsamen, M. C., Gerber-Wicht, C., and Lang, U. (2007) Prostaglandin E2 activates Stat3 in neonatal rat ventricular cardiomyocytes. A role in cardiac hypertrophy. *Cardiovasc. Res.* **73,** 57–65
28. Siddiquee, K., Zhang, S., Guida, W. C., Blaskovich, M. A., Greedy, B., Lawrence, H. R., Yip, M. L., Jove, R., McLaughlin, M. M., Lawrence, N. J., Sebti, S. M., and Turkson, J. (2007) Selective chemical probe inhibitor of Stat3, identified through structure-based virtual screening, induces antitumor activity. *Proc. Natl. Acad. Sci. U.S.A.* **104,** 7391–7396
29. Lin, L., Amin, R., Gallicano, G. I., Glasgow, E., Jogunoori, W., Jessup, J. M., Zasloff, M., Marshall, J. L., Shetty, K., Johnson, L., Mishra, L., and He, A. R. (2009) The STAT3 inhibitor NSC 74859 is effective in hepatocellular cancers with disrupted TGF-β signaling. *Oncogene* **28,** 961–972
30. Terui, K., Haga, S., Enosawa, S., Ohnuma, N., and Ozaki, M. (2004) Hypoxia/re-oxygenation-induced, redox-dependent activation of STAT1 (signal transducer and activator of transcription 1) confers resistance to apoptotic cell death via hsp70 induction. *Biochem. J.* **380,** 203–209
31. Daniels, A., van Bilsen, M., Goldschmeding, R., van der Vusse, G. J., and van Nieuwenhoven, F. A. (2009) Connective tissue growth factor and cardiac fibrosis. *Acta Physiol.* (*Oxf*) **195,** 321–338
32. Hedayat, M., Mahmoudi, M. J., Rose, N. R., and Rezaei, N. (2010) Proinflammatory cytokines in heart failure. Double-edged swords. *Heart Fail. Rev.* **15,** 543–562
33. Rohini, A., Agrawal, N., Koyani, C. N., and Singh, R. (2010) Molecular targets and regulators of cardiac hypertrophy. *Pharmacol. Res.* **61,** 269–280
34. Pan, J., Fukuda, K., Saito, M., Matsuzaki, J., Kodama, H., Sano, M., Takahashi, T., Kato, T., and Ogawa, S. (1999) Mechanical stretch activates the JAK/STAT pathway in rat cardiomyocytes. *Circ. Res.* **84,** 1127–1136
35. Takeda, K., Noguchi, K., Shi, W., Tanaka, T., Matsumoto, M., Yoshida, N., Kishimoto, T., and Akira, S. (1997) Targeted disruption of the mouse Stat3 gene leads to early embryonic lethality. *Proc. Natl. Acad. Sci. U.S.A.* **94,** 3801–3804
36. Hilfiker-Kleiner, D., Hilfiker, A., Fuchs, M., Kaminski, K., Schaefer, A., Schieffer, B., Hillmer, A., Schmiedl, A., Ding, Z., Podewski, E., Podewski, E., Poli, V., Schneider, M. D., Schulz, R., Park, J. K., Wollert, K. C., and Drexler, H. (2004) Signal transducer and activator of transcription 3 is required for myocardial capillary growth, control of interstitial matrix deposition, and heart protection from ischemic injury. *Circ. Res.* **95,** 187–195
37. Oshima, Y., Fujio, Y., Nakanishi, T., Itoh, N., Yamamoto, Y., Negoro, S., Tanaka, K., Kishimoto, T., Kawase, I., and Azuma, J. (2005) STAT3 mediates cardioprotection against ischemia/reperfusion injury through metallothionein induction in the heart. *Cardiovasc. Res.* **65,** 428–435
38. Negoro, S., Kunisada, K., Fujio, Y., Funamoto, M., Darville, M. I., Eizirik, D. L., Osugi, T., Izumi, M., Oshima, Y., Nakaoka, Y., Hirota, H., Kishimoto, T., and Yamauchi-Takihara, K. (2001) Activation of signal transducer and activator of transcription 3 protects cardiomyocytes from hypoxia/reoxygenation-induced oxidative stress through the up-regulation of manganese superoxide dismutase. *Circulation* **104,** 979–981
39. Podewski, E. K., Hilfiker-Kleiner, D., Hilfiker, A., Morawietz, H., Lichtenberg, A., Wollert, K. C., and Drexler, H. (2003) Alterations in Janus kinase (JAK) signal transducers and activators of transcription (STAT) signaling in patients with end stage-dilated cardiomyopathy. *Circulation* **107,** 798–802
40. Stephanou, A., Brar, B. K., Scarabelli, T. M., Jonassen, A. K., Yellon, D. M., Marber, M. S., Knight, R. A., and Latchman, D. S. (2000) Ischemia-induced STAT-1 expression and activation play a critical role in cardiomyocyte apoptosis. *J. Biol. Chem.* **275,** 10002–10008
41. Shen, Y., Devgan, G., Darnell, J. E., Jr., and Bromberg, J. F. (2001) Constitutively activated Stat3 protects fibroblasts from serum withdrawal and UV-induced apoptosis and antagonizes the proapoptotic effects of activated Stat1. *Proc. Natl. Acad. Sci. U.S.A.* **98,** 1543–1548
42. Ramires, F. J., Sun, Y., and Weber K. T. (1998) Myocardial fibrosis associated with aldosterone or angiotensin II administration. Attenuation by calcium channel blockade. *J. Mol. Cell. Cardiol.* **30,** 475–483
43. Hocher, B., Godes, M., Olivier, J., Weil, J., Eschenhagen, T., Slowinski, T., Neumayer, H. H., Bauer, C., Paul, M., and Pinto, Y. M. (2002) Inhibition of left ventricular fibrosis by tranilast in rats with renovascular hypertension. *J. Hypertens.* **20,** 745–751
44. Jia, N., Dong, P., Ye, Y., Qian, C., and Dai, Q. (2010) Allopurinol attenuates oxidative stress and cardiac fibrosis in angiotensin II-induced cardiac diastolic dysfunction. *Cardiovasc. Ther.*, in press
45. Törnig, J., Amann, K., Ritz, E., Nichols, C., Zeier, M., and Mall, G. (1996) Arteriolar wall thickening, capillary rarefaction, and interstitial fibrosis in the heart of rats with renal failure. The effects of ramipril, nifedipine, and moxonidine. *J. Am. Soc. Nephrol.* **7,** 667–675
46. Tyralla, K., Adamczak, M., Benz, K., Campean, V., Gross, M. L., Hilgers, K. F., Ritz, E., and Amann, K. (2011) High dose enalapril treatment reverses myocardial fibrosis in experimental uremic cardiomyopathy. *PLoS. One* **6,** e15287
47. Chen, L. M., Kuo, W. W., Yang, J. J., Wang, S. G., Yeh, Y. L., Tsai, F. J., Ho, Y. J., Chang, M. H., Huang, C. Y., and Lee, S. D. (2007) Eccentric cardiac hypertrophy was induced by long term intermittent hypoxia in rats. *Exp. Physiol.* **92,** 409–416
48. Yahata, Y., Shirakata, Y., Tokumaru, S., Yamasaki, K., Sayama, K., Hanakawa, Y., Detmar, M., and Hashimoto, K. (2003) Nuclear translocation of phosphorylated STAT3 is essential for vascular endothelial growth factor-induced human dermal microvascular endothelial cell migration and tube formation. *J. Biol. Chem.* **278,** 40026–40031
49. Battle, T. E., Lynch, R. A., and Frank, D. A. (2006) Signal transducer and activator of transcription 1 activation in endothelial cells is a negative regulator of angiogenesis. *Cancer Res.* **66,** 3649–3657
50. Vatner, D. E., Yang, G. P., Geng, Y. J., Asai, K., and Yun, J. S. (2000) Determinants of the cardiomyopathic phenotype in chimeric mice overexpressing cardiac $G\alpha_s$. *Circ. Res.* **86,** 802–806
51. Cook, S. A., Sugden, P. H., and Clerk, A. (1999) Activation of c-Jun N-terminal kinases and p38-mitogen-activated protein kinases in human heart failure secondary to ischaemic heart disease. *J. Mol. Cell. Cardiol.* **31,** 1429–1434
52. Behr, T. M., Nerurkar, S. S., Nelson, A. H., Coatney, R. W., Woods, T. N., Sulpizio, A., Chandra, S., Brooks, D. P., Kumar, S., Lee, J. C., Ohlstein, E. H., Angermann, C. E., Adams, J. L., Sisko, J., Sackner-Bernstein, J. D., and Willette, R. N. (2001) Hypertensive end-organ damage and premature mortality are p38 mitogen-activated protein kinase-dependent in a rat model of cardiac hypertrophy and dysfunction. *Circulation* **104,** 1292–1298
53. Takeishi, Y., Huang, Q., Abe, J., Glassman, M., Che, W., Lee, J. D., Kawakatsu, H., Lawrence, E. G., Hoit, B. D., Berk, B. C., and Walsh, R. A. (2001) Src and multiple MAP kinase activation in cardiac hypertrophy and congestive heart failure under chronic pressure-overload. Comparison with acute mechanical stretch. *J. Mol. Cell. Cardiol.* **33,** 1637–1648
54. Bueno, O. F., De Windt, L. J., Lim, H. W., Tymitz, K. M., Witt, S. A.,

Kimball, T. R., and Molkentin, J. D. (2001) The dual-specificity phosphatase MKP-1 limits the cardiac hypertrophic response *in vitro* and *in vivo*. *Circ. Res.* **88,** 88–96

55. Xiao, L., Pimental, D. R., Amin, J. K., Singh, K., Sawyer, D. B., and Colucci, W. S. (2001) MEK1/2-ERK1/2 mediates α1-adrenergic receptor-stimulated hypertrophy in adult rat ventricular myocytes. *J. Mol. Cell. Cardiol.* **33,** 779–787
56. Bueno, O. F., and Molkentin, J. D. (2002) Involvement of extracellular signal-regulated kinases 1/2 in cardiac hypertrophy and cell death. *Circ. Res.* **91,** 776–781
57. Skoumal, R., Tóth, M., Serpi, R., Rysä, J., Leskinen, H., Ulvila, J., Saiho, T., Aro, J., Ruskoaho, H., Szokodi, I., and Kerkelä, R. (2011) Parthenolide inhibits STAT3 signaling and attenuates angiotensin II-induced left ventricular hypertrophy via modulation of fibroblast activity. *J. Mol. Cell. Cardiol.* **50,** 634–641
58. Kleinbongard, P., Heusch, G., and Schulz, R. (2010) TNFα in atherosclerosis, myocardial ischemia/reperfusion, and heart failure. *Pharmacol. Ther.* **127,** 295–314